Supplementary Information

Guanidyl-implanted UiO-66 as efficient catalysts for enhanced conversion of carbon dioxide into cyclic carbonates

Aijia Gao,[a] Fangfang Li,[a] Zhi Xu,[a] Changchun Ji,[a] Jing Gu,[*b] and Ying-Hua Zhou[*a]

[a] The Key Laboratory of Functional Molecular Solids, Ministry of Education, Anhui Laboratory of Molecule-Based Materials, College of Chemistry and Materials Science, Anhui Normal University, Wuhu, Anhui 241002, China
[b] Department of Chemistry and Biochemistry, San Diego State University, San Diego State University

E-mail: yhzhou@ahnu.edu.cn; jgu@sdsu.edu

Table S1 Comparison of the catalytic performance of UiO-66-Gua$_{0.2}$(s) with previously reported MOFs.

Entry	Catalyst	Epoxide	Cocatalyst (mol%)	Time (h)	T (℃)	P (MPa)	Yield	Ref.
1	USTC-253-TFA	PO	6.5	72	25	0.1	38.2%	1
2	PS/UiO-66 fiber	ECH	1.55	4	120	2	78%	2
3	PVA/UiO-66 fiber	ECH	1.55	4	120	2	71%	2
4	MOF-5-NH$_2$	ECH	0.5	6	50	1.2	81%	3
5	UiO-66/Cu-BTC	PO	0.5	6	60	1.2	88%	4
6	UMCM-1-NH$_2$	PO	0.44	24	RT	1.2	90%	5
7	PNU-25-NH$_2$	PO	0.5	18	55	0.1	93%	6
8	UiO-66-Gua$_{0.2}$(s)	ECH	0.8	12	70	0.1	84%	This work
9	UiO-66-Gua$_{0.2}$(s)	PO	0.8	12	70	0.1	96%	This work

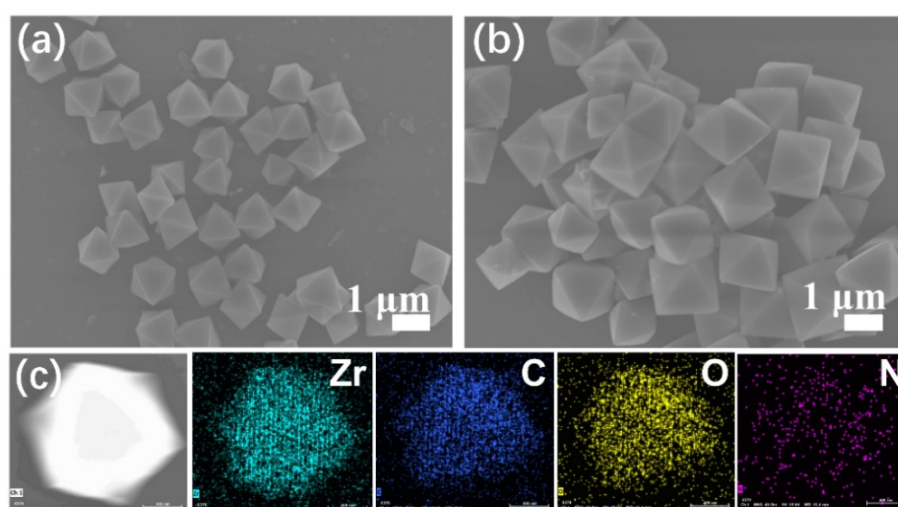Note：PO = propylene oxide; ECH = epichlorohydrin.

Fig. S1 SEM images of (a) UiO-66(l) and (b) UiO-66-Gua$_{0.2}$(l). (c) SEM image of UiO-66-Gua$_{0.2}$(l) particle slice and corresponding elemental mapping of Zr, C, O, and N, respectively.
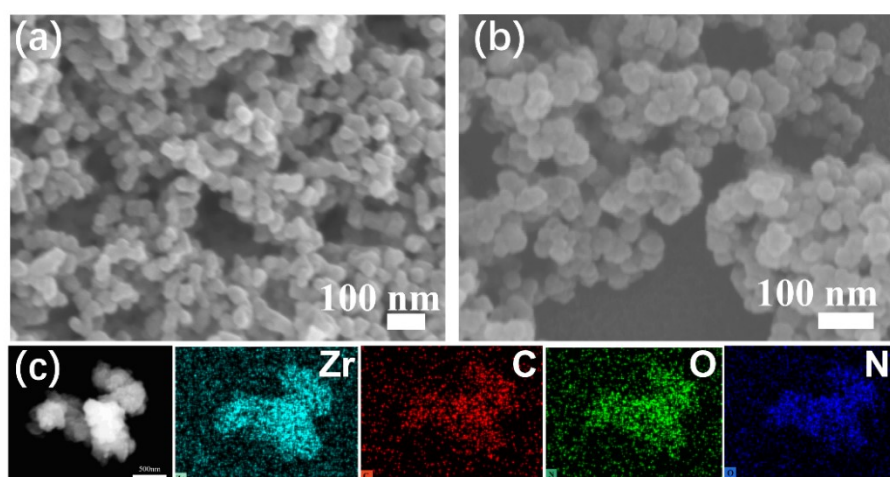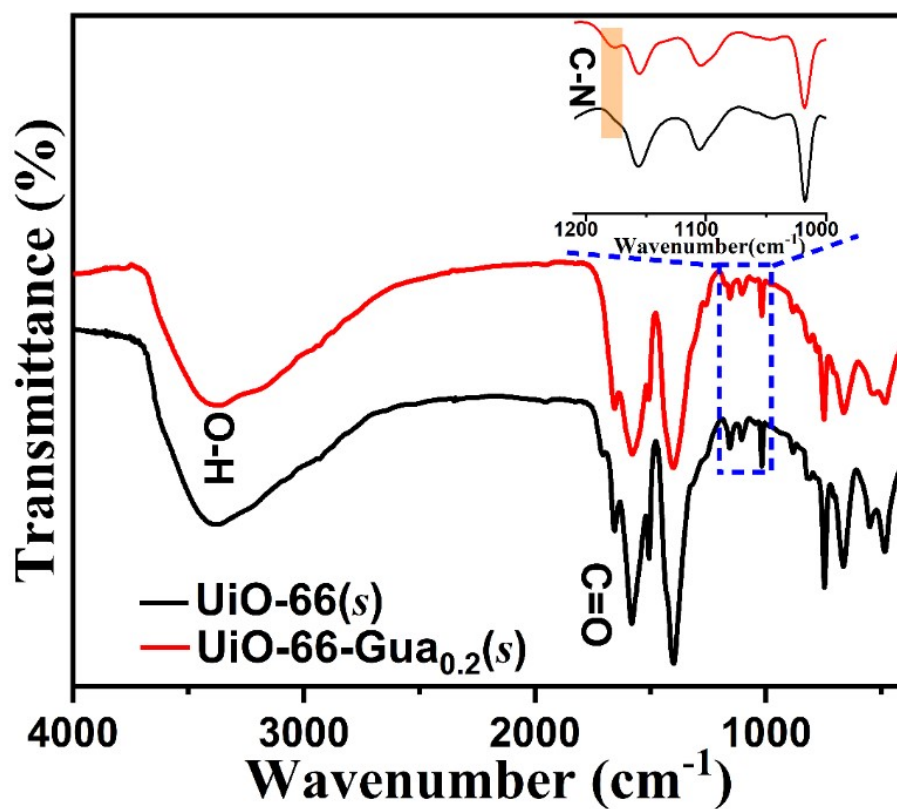

Fig. S2 SEM images of (a) UiO-66(s) and (b) UiO-66-Gua$_{0.2}$(s). (c) SEM image of UiO-66-Gua$_{0.2}$(s) particle slice and corresponding elemental mapping of Zr, C, O, and N, respectively.

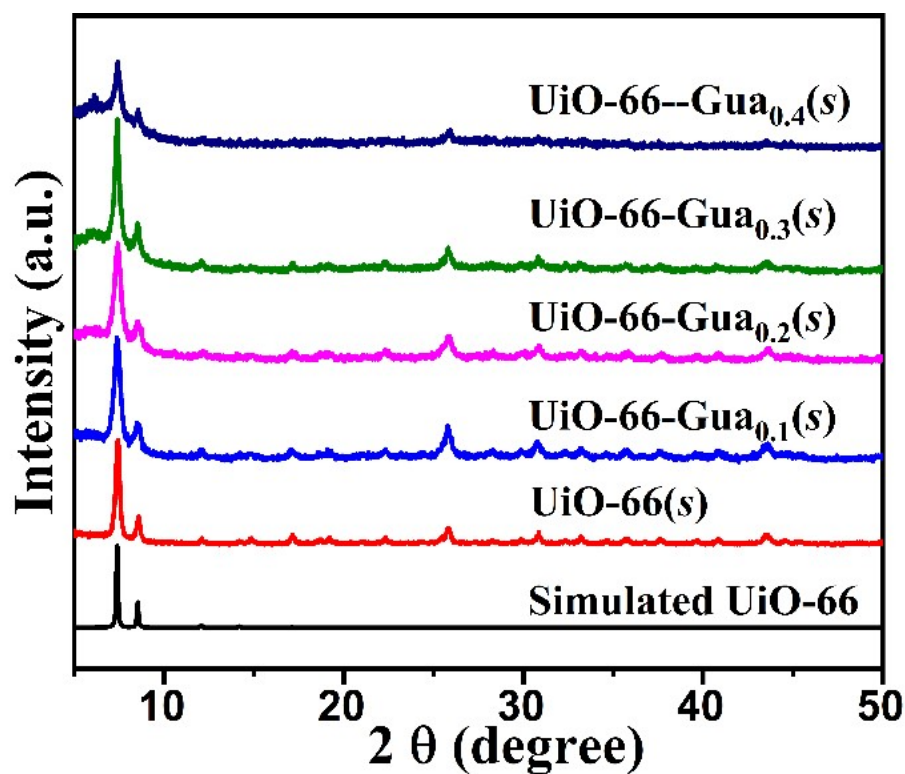**Fig. S3** FT-IR spectra of UiO-66(s) and UiO-66-Gua$_{0.2}$(s).

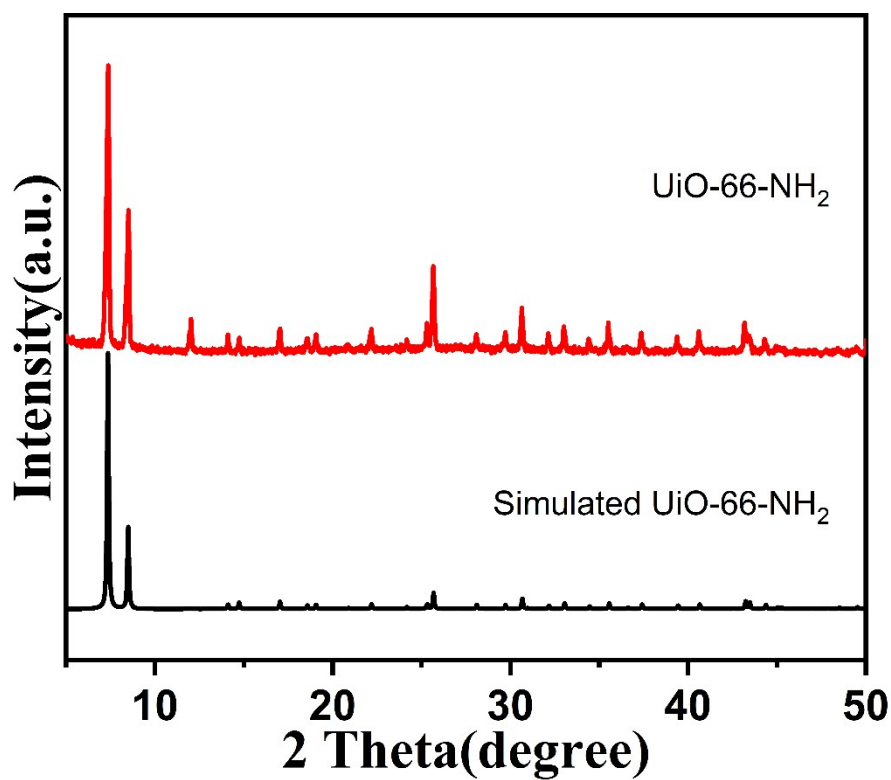**Fig. S4** PXRD patterns of UiO-66-Gua$_x$(s) with different amount of 4-guanidinobenzoic acid hydrochloride (Gua).
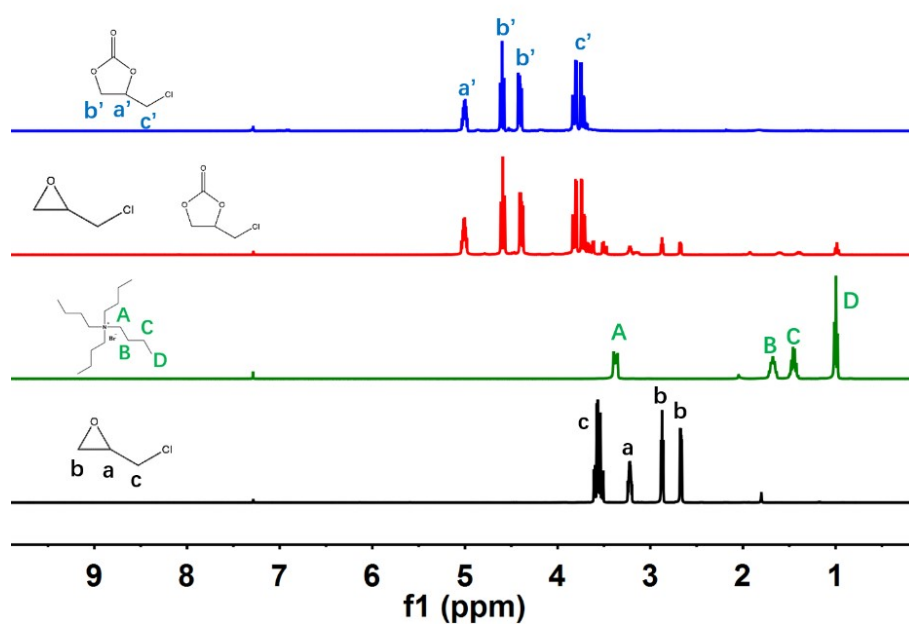
Fig. S5 PXRD pattern of UiO-66-NH$_2$.

Fig. S6 ^{1}H-NMR spectra (CDCl$_3$) for CO$_2$ cycloaddition with epichlorohydrin using UiO-66-Gua$_{0.2}$(*s*) catalyst. Black line: the substrate; Green line: TBAB; Red line: the reaction solution after centrifugation (conditions: 10 mg catalyst, 0.8 mol% TBAB, 1.0 atm CO$_2$ and 70 °C for 12 h); Blue line: the isolated product.
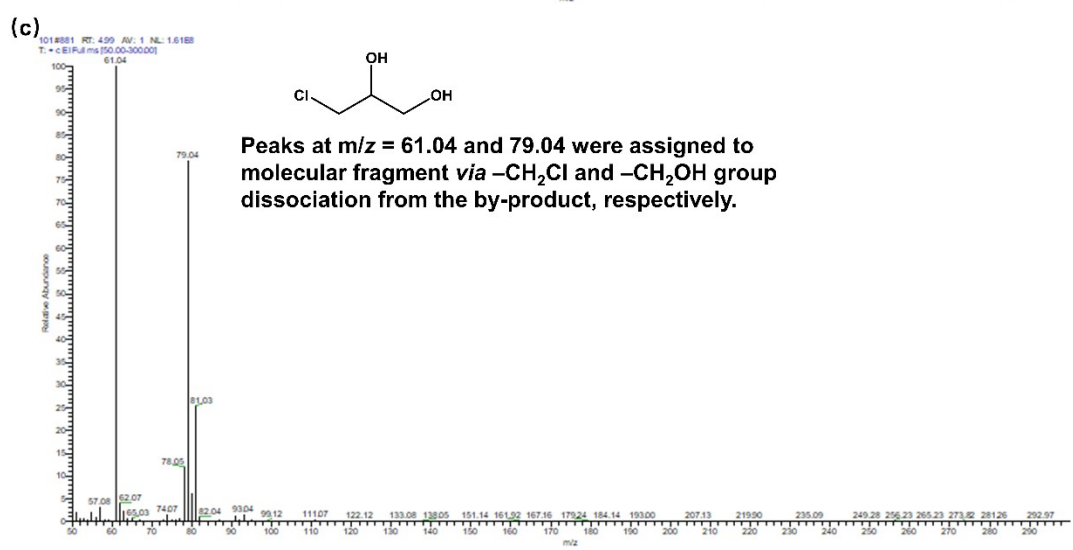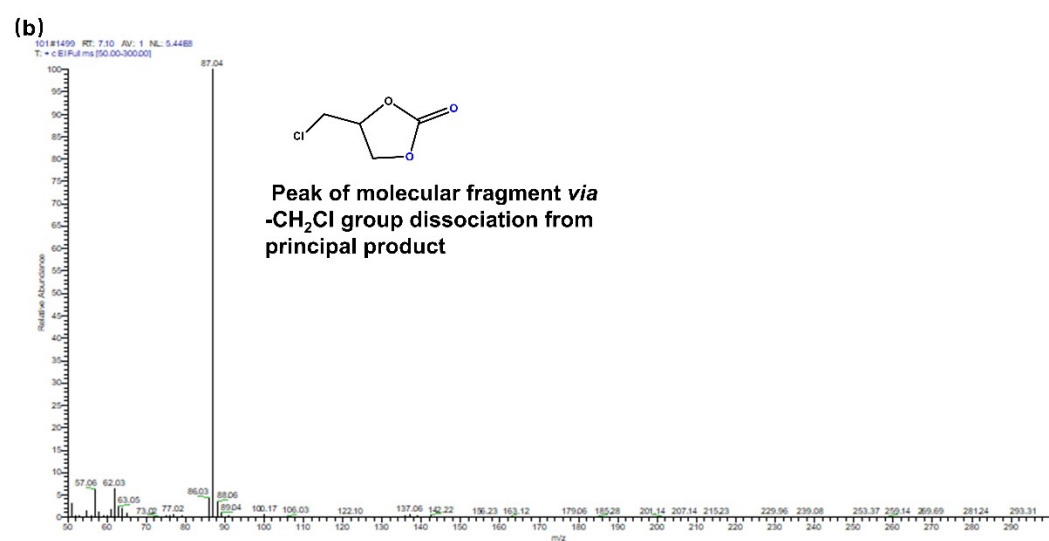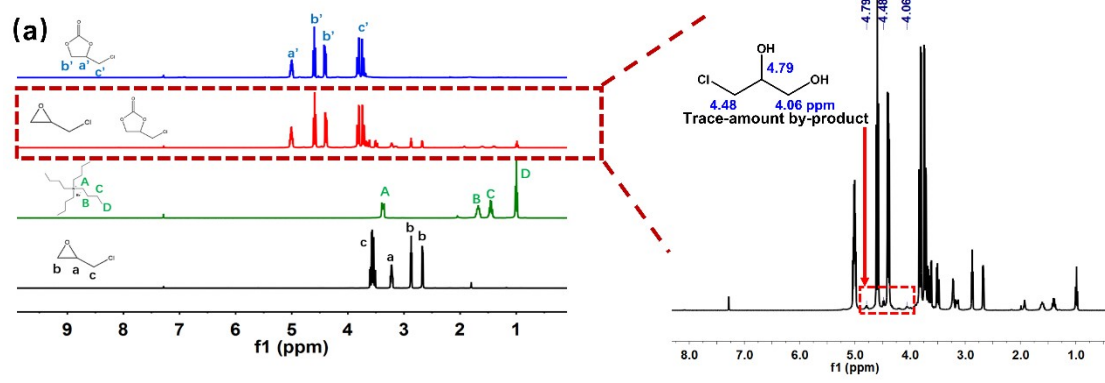
Fig. S7 (a) ^{1}H-NMR (a) spectra (CDCl$_3$) for CO$_2$ cycloaddition with epichlorohydrin using UiO-66-Gua$_{0.2}$(*s*) catalyst (conditions: 10 mg catalyst, 0.8 mol% TBAB, 1.0 atm CO$_2$ and 70 ˚C for 12 h); (b) mass spectra of the principal product; (c) mass spectra of the by-product.
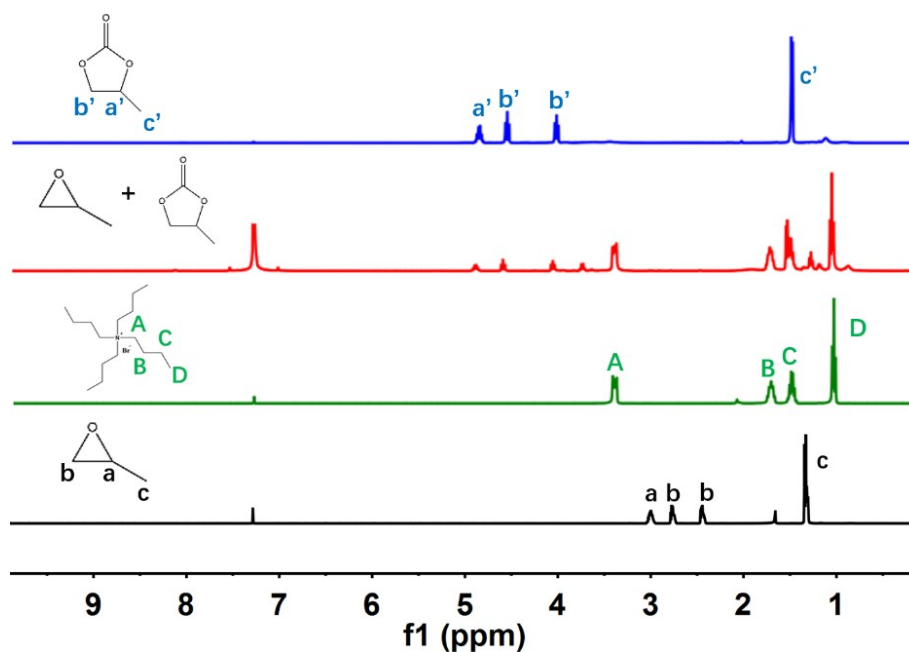
Fig. S8 ^{1}H-NMR spectra ($CDCl_3$) for CO_2 cycloaddition with propylene oxide using UiO-66-Gua$_{0.2}$(*s*) catalyst. Black line: the substrate; Green line: TBAB; Red line: the reaction solution after centrifugation (conditions: 10 mg catalyst, 0.8 mol% TBAB, 1.0 atm CO_2 and 70 ˚C for 12 h); Blue line: the isolated product.

Fig. S9 ^{1}H-NMR spectra ($CDCl_3$) for CO_2 cycloaddition with epibromohydrin using UiO-66-Gua$_{0.2}$(*s*) catalyst. Black line: the substrate; Green line: TBAB; Red line: the reaction solution after centrifugation (conditions: 10 mg catalyst, 0.8 mol% TBAB, 1.0 atm CO_2 and 70 ˚C for 12 h); Blue line: the isolated product.
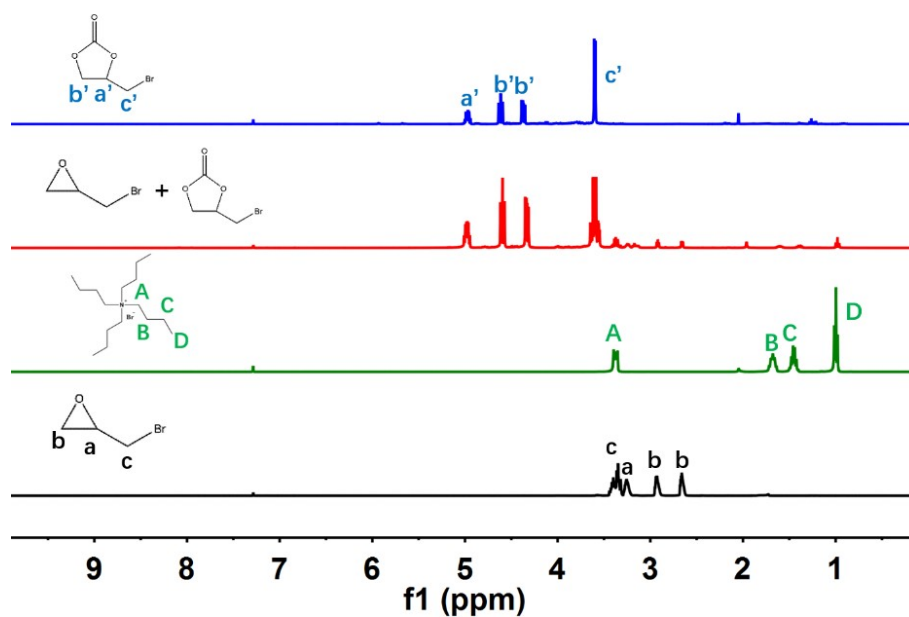
Fig. S10 ^{1}H-NMR spectra (CDCl$_3$) for CO$_2$ cycloaddition with 1,2-epoxyhexane using UiO-66-Gua$_{0.2}$(*s*) catalyst. Black line: the substrate; Green line: TBAB; Red line: the reaction solution after centrifugation (conditions: 10 mg catalyst, 0.8 mol% TBAB, 1.0 atm CO$_2$ and 70 ˚C for 12 h); Blue line: the isolated product.

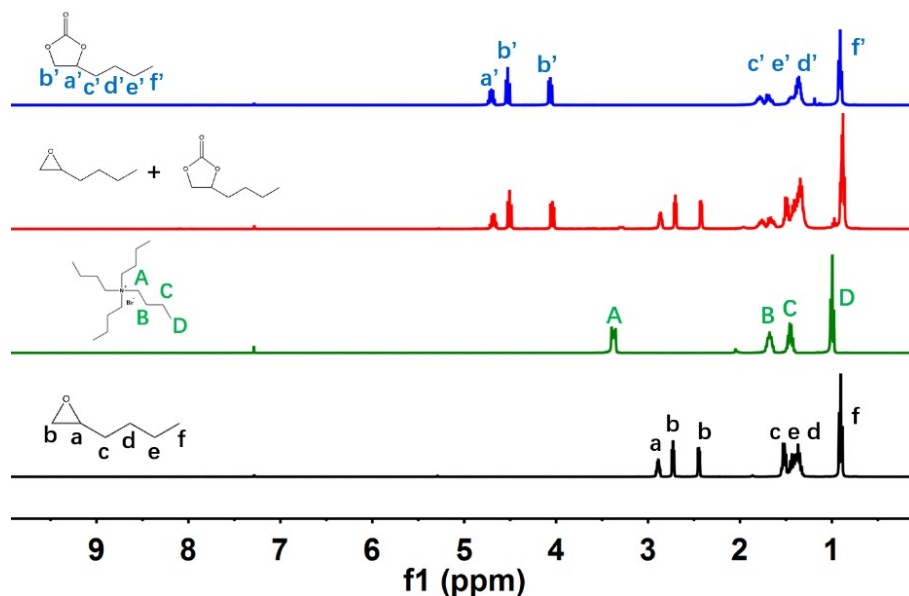**Fig. S11** ^{1}H-NMR spectra (CDCl$_3$) for CO$_2$ cycloaddition with epoxypropyl phenyl ether using UiO-66-Gua$_{0.2}$(*s*) catalyst. Black line: the substrate; Green line: TBAB; Red line: the reaction solution after centrifugation (conditions: 10 mg catalyst, 0.8 mol% TBAB, 1.0 atm CO$_2$ and 70 ˚C for 12 h); Blue line: the isolated product.
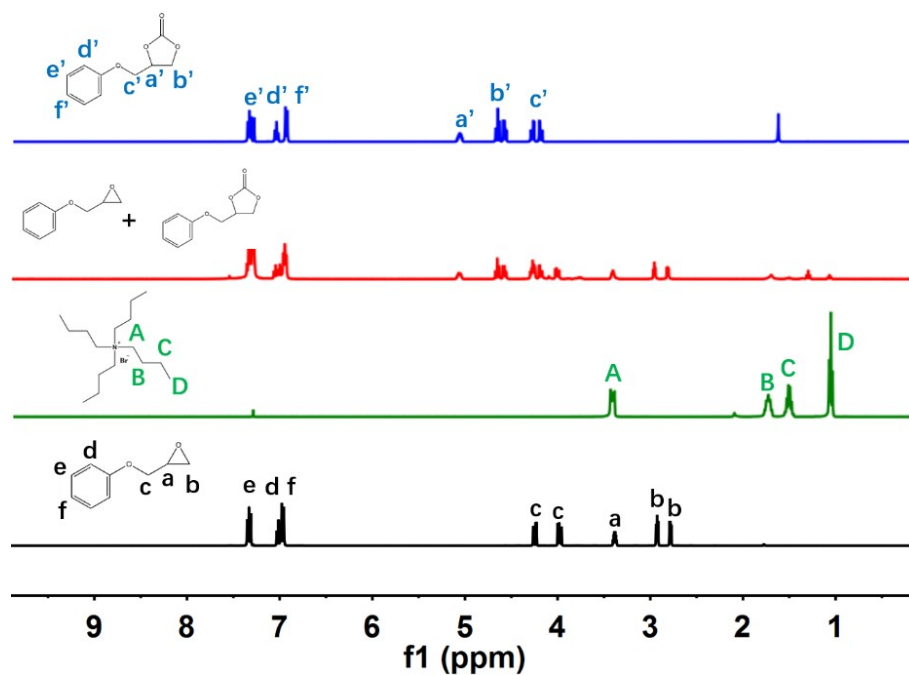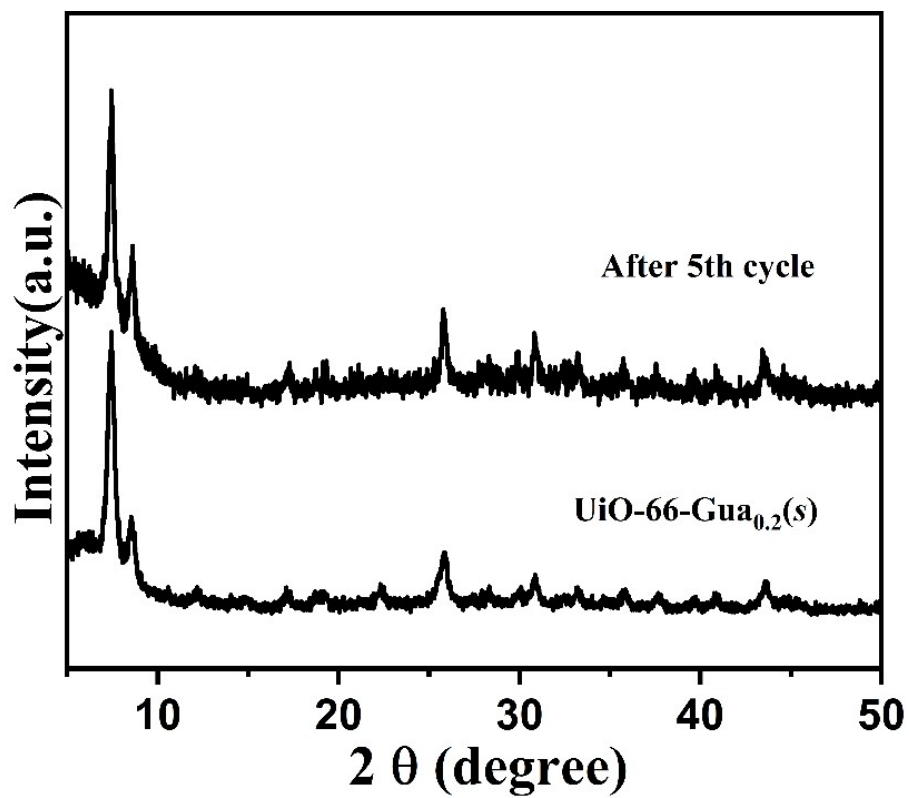
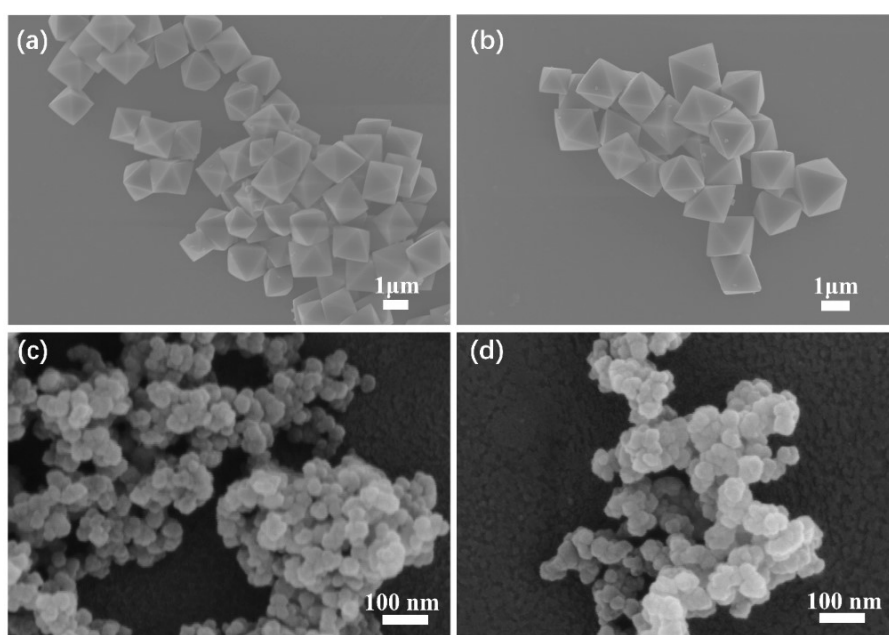**Fig. S12** PXRD patterns of UiO-66-Gua$_{0.2}$(*s*) before and after five catalytic cycles.

Fig. S13 SEM images of (a) as-synthesized UiO-66-Gua$_{0.2}$(*l*), (b) UiO-66-Gua$_{0.2}$(*l*) after catalytic cycles, (c) as-synthesized UiO-66-Gua$_{0.2}$(*s*), and (d) UiO-66-Gua$_{0.2}$(*s*) after catalytic cycles.

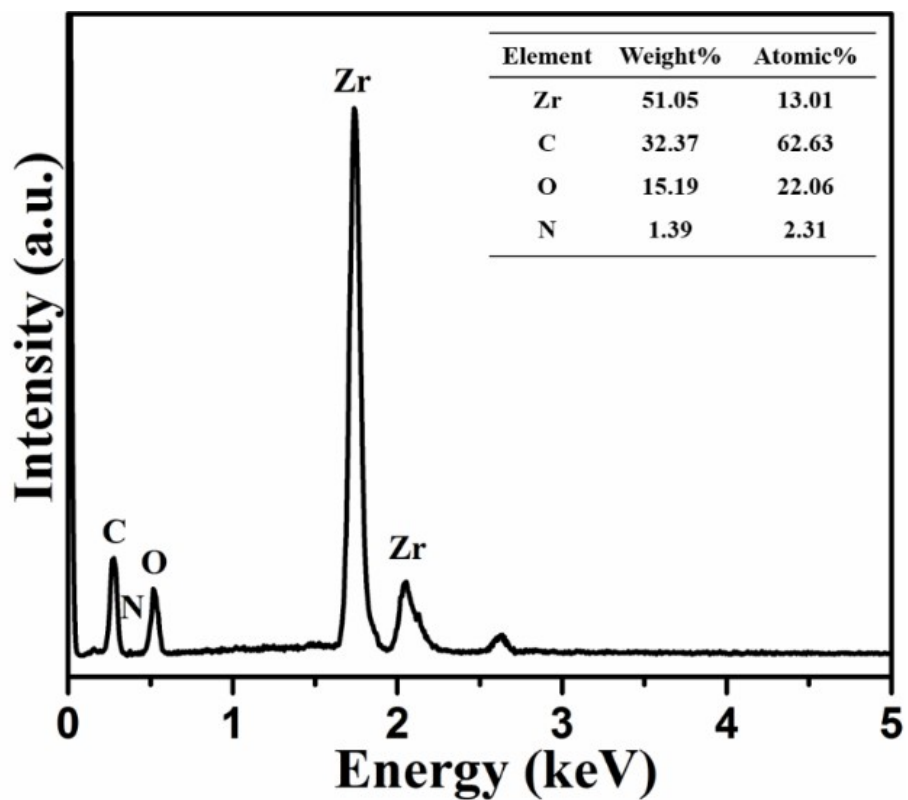| Element	Weight%	Atomic%
Zr	51.05	13.01
C	32.37	62.63
O	15.19	22.06
N	1.39	2.31

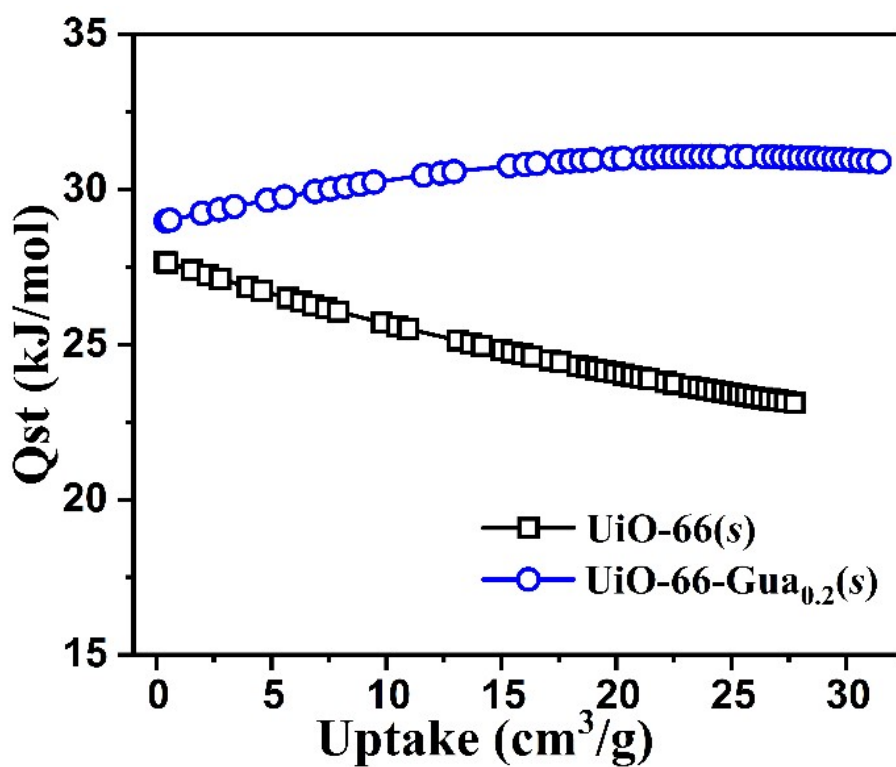**Fig. S14** EDS pattern of UiO-66-Gua$_{0.2}$(*s*) after catalysis.

Fig. S15 CO$_2$ adsorption heat (Qst) for UiO-66(*s*) and UiO-66-Gua$_{0.2}$(*s*).
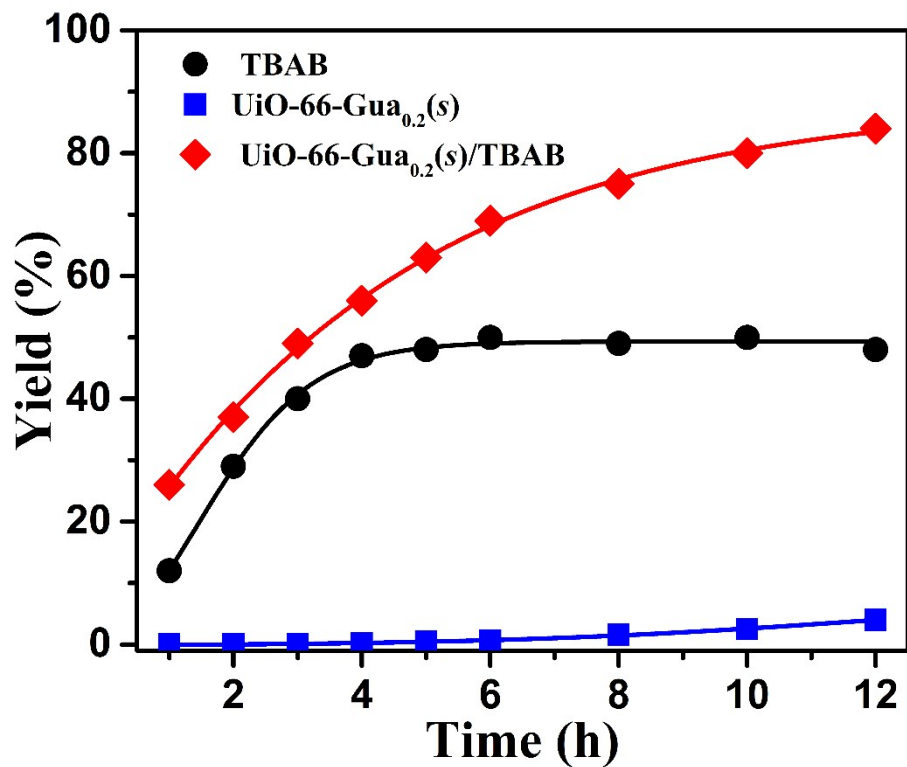
Fig. S16 The plot of the yield versus time in the presence of UiO-66-Gua$_{0.2}$(*s*), TBAB and UiO-66-Gua$_{0.2}$(*s*)/TBAB.
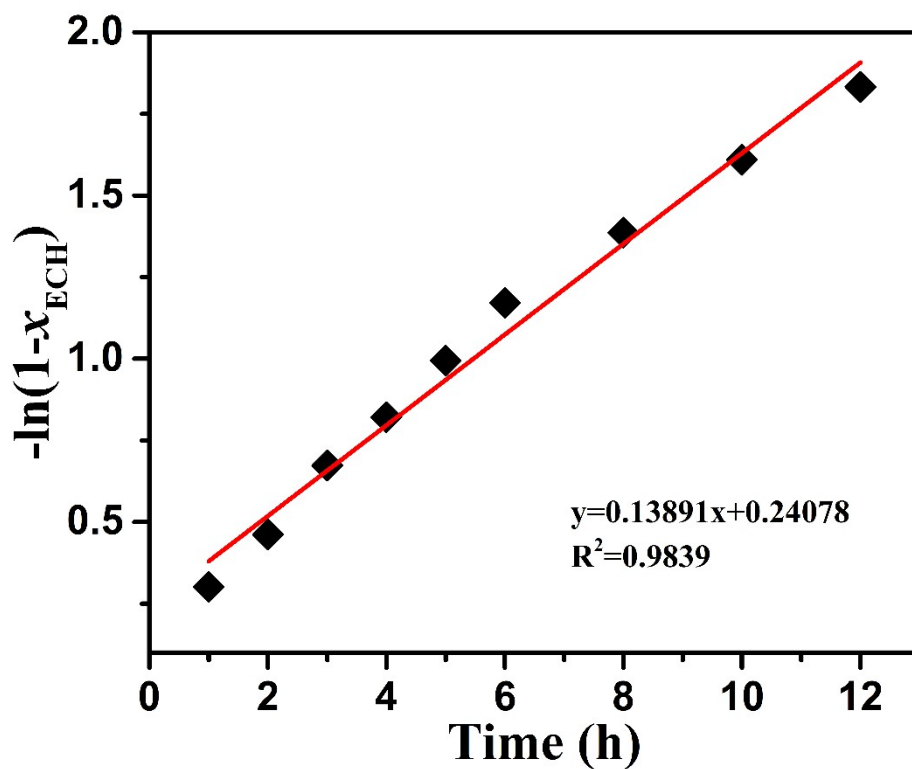

Fig. S17 First-order kinetic plot of the –ln(1-x_{ECH}) versus time in the presence of UiO-66-Gua$_{0.2}$(*s*)/TBAB.

The reaction kinetic of CO_2 cycloaddition to epichlorohydrin (ECH) was studied by using a reported approach. The following rate Eq. S1 is used in calculating the kinetics of this reaction:

$$rate = -d[ECH]/dt = k\,(ECH)^a\,(CO_2)^b\,(catalyst)^c\,(cocatalyst)^d \qquad (S1)$$

Here the k is the rate constant.

Since the amount of CO_2 is in excess hence its pressure could be considered as constant, moreover the amount of catalyst (10 mg) and cocatalyst (0.8 mol%) could be considered constant as their concentrations are not changing throughout the reaction. So the above Eq. S1 could be reduced to following Eq. S2

$$rate = -d[ECH]/dt = k_{obs}\,(ECH)^a \qquad (S2)$$

Where $k_{obs} = k\,(CO_2)^b\,(catalyst)^c\,(cocatalyst)^d$,

$$(ECH) = (ECH)_0 \times (1\text{-}x_{ECH})$$

k_{obs} was the observed *quasi*-first-order rate constant for ECH concentration. And x_{ECH} was the conversion percentage of ECH. From Eq. S2 it was clear that the rate of reaction depends only on the concentration of ECH hence the reaction kinetic is determined only with respect to the substrate of ECH. Eq. S2 was converted to Eq. S3 by the integral as following.

$$-\ln(1 - x_{ECH}) = k_{obs} \cdot t \qquad (S3)$$

From the curve of $-\ln(1 - x_{ECH})$ vs time were linearly fitted by the Eq. S3, the k_{obs} value for the *quasi*-first-order reaction was found to be 0.14 h^{-1}.

References:

S1 Z. R. Jiang, H. Wang, Y. Hu, J. Lu and H. L. Jiang, *ChemSusChem*, 2015, **8**, 878-885.

S2 R. Mirzaei, M. Bahadori, R. Kardanpour, S. Rafiei, S. Tangestaninejad, M. Moghadam, V. Mirkhani, I. Mohammadpoor-Baltork and S. E. Mirazimi, *Dalton Trans*, 2021, **50**, 10567-10579.

S3 J. F. Kurisingal, Y. Rachuri, Y. Gu, Y. Choe and D.-W. Park, *Chemical Engineering Journal*, 2020, **386**, 121700.

S4 J. F. Kurisingal, Y. Rachuri, Y. Gu, G.-H. Kim and D.-W. Park, *Applied Catalysis A: General*, 2019, **571**, 1-11.

S5 R. Babu, A. C. Kathalikkattil, R. Roshan, J. Tharun, D.-W. Kim and D.-W. Park, *Green Chemistry*, 2016, **18**, 232-242.

S6 J. F. Kurisingal, Y. Rachuri, Y. Gu, R. K. Chitumalla, S. Vuppala, J. Jang, K. K. Bisht, E. Suresh and D.-W. Park, *ACS Sustainable Chemistry & Engineering*, 2020, **8**, 10822-10832.